ChemComm

COMMUNICATION

View Article Online
View Journal | View Issue

Cite this: *Chem. Commun.*, 2020, **56**, 2320

Received 6th October 2019,
Accepted 18th December 2019

DOI: 10.1039/c9cc07845b

rsc.li/chemcomm

Biotinylated photoactive Pt(IV) anticancer complexes†

Huayun Shi, Cinzia Imberti, Huaiyi Huang, Ian Hands-Portman and Peter J. Sadler *

Novel biotinylated diazido-Pt(IV) complexes exhibit high visible light photocytotoxicity while being stable in the dark. Photocytotoxicity and cellular accumulation of all-*trans*-[Pt(py)$_2$(N$_3$)$_2$(biotin)(OH)] (2a) were enhanced significantly when bound to avidin; irradiation induced dramatic cellular morphological changes in human ovarian cancer cells treated with 2a.

Tumour-targeting drugs can improve selective drug delivery to cancer cells and reduce undesirable side effects.[1–4] Biotin (vitamin H or B7) plays an important role as cellular growth promoter and co-enzyme for carboxylase enzymes.[5] Exogenous biotin is taken up *via* a high-affinity biotin transporter and a sodium-dependent multivitamin transporter (SMVT).[6,7] Notably, cancer cells overexpress SMVT, thus making biotin a tumour-targeting vector.[8–10] Biotin possesses a high affinity specific for tetrameric egg white avidin through noncovalent bonding with K_d values of 10^{-13} to 10^{-15} M.[11] The avidin–biotin complex induces a relatively low immune response *in vivo* and has been widely used in cancer-targeted therapy.[5,12–15] Avidin displays strong adherence to cells *in vitro*, and can be administered as a nano-carrier for delivery of biotinylated drugs.[16] Biotinylation of drugs is therefore a feasible strategy to improve their cancer-cell accumulation and selectivity,[17,18] and has also been applied in the design of photoactive drugs.[19–22]

Photoactive Pt agents provide spatial control of cytotoxicity with novel mechanisms of action and lack of cross-resistance with cisplatin.[23,24] Diazido Pt(IV) complexes are potent photoactive prodrugs with high dark stability due to their kinetic inertness,[25–27] and photocytotoxicity exerted by the combined effects of Pt(II) products, azidyl radicals and reactive oxygen species (ROS) formed on photoactivation.[28–30] *Trans*,*trans*,*trans*-[Pt(N$_3$)$_2$(OH)$_2$(py)$_2$] (**1**) kills cancer cells upon irradiation with high photocytotoxicity (dark *versus* light) indices.[27] Axial OH ligands enhance aqueous solubility of Pt(IV) complexes and stabilise the Pt^{IV} oxidation state.[31] Derivatisation of the releasable axial ligand can improve the pharmacological properties without altering the mechanism of action.[32–34]

Herein, we have prepared two novel biotinylated diazido Pt(IV) complexes *trans*,*trans*,*trans*-[Pt(py)$_2$(N$_3$)$_2$(biotin)(OH)] (**2a**) and *trans*,*trans*,*trans*-[Pt(py)$_2$(N$_3$)$_2$(biotin)(DCA)] (**2b**, Scheme 1). The pyruvate dehydrogenase kinase (PDK) inhibitor dichloroacetate (DCA) can be delivered to cancer cells effectively as an axial ligand in Pt(IV) prodrugs.[35–37] Dark stability, photodecomposition, photoreactions with 5′-GMP and DNA, and interaction with avidin were investigated for **2a** and **2b**, and their photocytotoxicity and cellular accumulation compared to those of avidin-complex adducts. Cellular morphological changes upon treatment of cancer cells with **2a** were examined by confocal microscopy.

The synthetic routes for photoactive Pt(IV) complexes **2a** and **2b** are summarised in Scheme 1. Mono-substituted **2a** was obtained by combining **1** with biotin using TBTU/DIPEA as coupling agents, while the bi-substituted **2b** was synthesised by stirring **2a** with DCA anhydride. Both complexes gave satisfactory elemental analyses and were also characterised by ESI-HRMS, NMR and UV-vis spectroscopy, and for purity by HPLC (Fig. S1, ESI†).

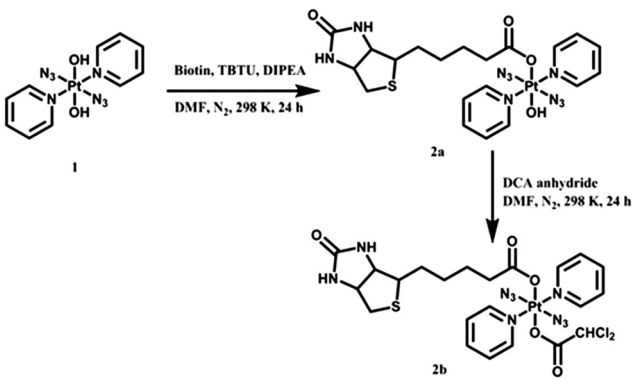

Scheme 1 Synthetic routes for biotinylated complexes **2a** and **2b**.

Department of Chemistry, University of Warwick, Coventry, CV4 7AL, UK.
E-mail: p.j.sadler@warwick.ac.uk

† Electronic supplementary information (ESI) available: NMR spectra, photodecomposition, UV-vis titration, and experimental details. See DOI: 10.1039/c9cc07845b

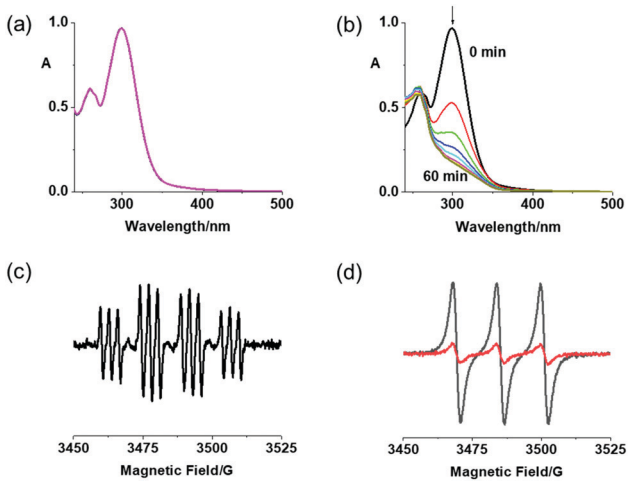

Fig. 1 (a) UV-vis spectral changes for **2a** (50 μM) in RPMI-1640 in the dark for 2 h, and (b) in H_2O upon 1 h irradiation with blue light (420 nm); (c) EPR spectra for **2a** (2.5 mM) with DMPO in H_2O after irradiation (463 nm), and (d) with TEMP in CH_3CN in the dark (—) and after irradiation (463 nm, —).

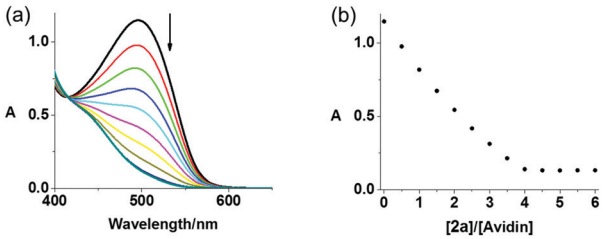

Fig. 2 (a) UV-vis spectral changes for avidin–HABA in PBS solution upon addition of complex **2a** in DMSO, (b) absorbance change at 496 nm in HABA displacement titrations of biotinylated complexes **2a**.

The ^{1}H and ^{13}C NMR data are consistent with the proposed structures of the complexes. The Pt-coordinated pyridine has characteristic ^{1}H NMR doublets with ^{195}Pt satellites at *ca.* 8.8 ppm, and the triplets at *ca.* 8. 3 and 7.9 ppm, with ^{13}C NMR resonances at *ca.* 150, 143 and 127 ppm (Fig. S2–S5, ESI†). Two typical singlets at 6.38 and 6.35 ppm assignable to NHC(O)NH of biotin were detected for both complexes. The electronic absorption spectra of **2a** and **2b** in aqueous solution were similar, although **2b** exhibited a slight red shift of the LMCT ($N_3 \rightarrow Pt$) transition and stronger absorption at wavelengths <270 nm due to the presence of the DCA ligand.

Complexes **2a** and **2b** exhibited excellent dark stability in RPMI-1640/DMSO (95%/5%, v/v) monitored by UV-vis spectroscopy (Fig. 1a and Fig. S6a, ESI†). When irradiated with blue light (420 nm), the LMCT bands of both complexes at *ca.* 300 nm decreased in intensity, indicating release of the azide ligands (Fig. 1b and Fig. S6b, ESI†).[27] Notably, **2b** exhibited a larger decrease at the absorption maximum, probably due to release of the DCA ligand. Released azidyl radicals and singlet oxygen were trapped by DMPO and TEMP, respectively, for **2a** upon irradiation (463 nm; Fig. 1c and d).

The photoreactions of **2a**/**2b** with 5′-GMP were analysed by LC-MS. Pt(IV) complexes (30 μM) were incubated with 5′-GMP (2 mol equiv.) at 310 K in the dark for 1 h, then irradiated by blue light (420 nm) for 1 h (Fig. S7, ESI†). For both complexes, $[Pt^{II}(CH_3CN)(py)_2(GMP\text{-}H)]^+$ (G1, 756.48 *m*/*z*) was detected as the major Pt-GMP product, together with two minor adducts $[Pt^{II}(HCOO)(py)_2(GMP)]^+$ (G2, 762.18 *m*/*z*) and $[Pt^{II}(N_3)(py)_2(GMP)]^+$ (G3, 758.23 *m*/*z*). These results were similar to those obtained for **1**, suggesting a negligible effect of axial substituents on the photoreaction with guanine.[38]

DNA melting experiments monitored by UV-vis were carried out in phosphate buffer (1 mM, pH = 7.9) to investigate DNA binding with a drug/base pair ratio of 0.2 (Table S1, ESI†). Similar to parent complex **1**, **2a** and **2b** interact with ct-DNA only weakly (ΔT_m < 2 K) in the dark, while upon irradiation with blue light (420 nm) an apparent interaction was observed (ΔT_m *ca.* 5 K). The increase in the DNA melting temperature suggests that **2a** and **2b** might form inter-strand cross-links after irradiation, similar to **1**.

The binding affinity of avidin towards **2a** and **2b** in PBS was assessed by a displacement titration using HABA (2-(4-hydroxyphenylazo)benzoic acid) and monitored by UV-vis spectroscopy (Fig. 2). The avidin–HABA adduct displays an absorption band at *ca.* 496 nm, which decreases when HABA is replaced by biotin.[39] On mixing, a gradual decrease of the absorbance at 496 nm was observed upon addition of either complex to a solution containing HABA (160 μM) and avidin (8 μM), indicating their stronger binding to avidin compared with HABA (dissociation constant $K_d = 10^{-6}$ M).[39] A sharp end point and same absorbance changes ($\Delta A = 1.01$) with biotin were observed for **2a** and **2b**, indicating their similar affinity towards avidin as unmodified biotin. These results suggested the possibility of using avidin as a nanocarrier for delivery of biotinylated complexes to cancer cells.

The IC_{50} values of **2a** and **2b** in human A2780 ovarian, A549 lung and PC3 prostate cancer cell lines were determined by the sulforhodamine B (SRB) colorimetric assay (Table 1), using parent complex **1** and **CDDP** (cisplatin) as references. Both complexes were relatively non-toxic towards all cancer cells and healthy MRC-5 lung fibroblasts in the dark with IC_{50} values >50/100 μM, but exhibited promising photocytotoxicity with high photocytotoxicity indices (PI). In all the cancer cell lines studied, di-substituted **2b** (1.3–5.9 μM) is at least twice as phototoxic as the mono-substituted **2a** (11.7–21.1 μM), and 5× more toxic than **1** (7.1–55.6 μM). Under the same conditions, cisplatin exhibited very low cytotoxicity in all cell lines (IC_{50} > 100 μM) due to the short incubation time (2 h).

In A2780 ovarian cancer cells, **2a** (IC_{50} = 11.7 μM) was slightly less active than **1** (IC_{50} = 7.1 μM), while **2b** was more potent (IC_{50} = 1.3 μM), potentially attributable to the synergistic anticancer activity of the released DCA ligand. In order to investigate the effect of avidin on activity, **2a** was mixed with avidin (**2a** : avidin = 4 : 1) prior to addition to A2780 cells following the same protocol used for **2a** alone. Notably, the avidin–**2a** complex exhibited good dark stability, being potently photocytotoxic in A2780 cells with an IC_{50} value of 4.4 μM, 2.7× lower than that of **2a**, and 1.6× more toxic than **1**. In contrast, the photocytotoxicity of **2b** was not enhanced in the presence of avidin.

Table 1 IC_{50} values and photocytotoxicity indices (PI) for **2a** and **2b** obtained after 1 h incubation, 1 h irradiation (465 nm) and 24 h recovery, in comparison with the parent complex **1** and **CDDP** (cisplatin)[34]

		Cell line/IC_{50} (μM)[a]			
Comp.		A2780	A549	PC3	MRC5
2a	Dark	>100	>100	>100	>100
	Irrad	11.7 ± 0.3	13.3 ± 0.7	21.1 ± 0.4	
	PI	>8.5	>7.5	>4.7	
2a–avi (4 : 1)	Dark	>100			
	Irrad	4.4 ± 0.3			
	PI	>22.7			
2b	Dark	>50	>100	>100	>100
	Irrad	1.3 ± 0.2	5.9 ± 0.6	3.0 ± 0.1	
	PI	>38.5	>16.9	>33.3	
2b–avi (4 : 1)	Dark	>50			
	Irrad	2.45 ± 0.01			
	PI	>20.4			
1	Dark	>100	>100	>100	>100
	Irrad	7.1 ± 0.4	51.9 ± 2.5	55.6 ± 0.9	
	PI	>14.1	>1.9	>1.8	
CDDP	Dark	>100	>100	>100	>100
	Irrad	>100	>100	>100	

[a] Data are from three independent experiments.

Since biotin is expected to exhibit a preference towards cancer cells due to overexpressed receptors,[5] ICP-MS was used to quantify and compare the cellular uptake of biotinylated complexes **2a** and **2b** as well as the unsubstituted **1**. A2780 ovarian cancer cells were treated with 10 μM prodrugs in the dark for 1 h, then the Pt content of cells was analysed by ICP-MS (Table 2). The mono-substituted **2a** exhibited lower Pt accumulation (0.4 ng per 10^6 cells) than **1** (0.64 ng per 10^6 cells) after 1 h incubation, while accumulation of di-substituted **2b** (21.1 ng per 10^6 cells) was 33× higher than that of **1** and 53× higher than **2a**. These results showed that conjugation with biotin alone did not increase the accumulation of diazido Pt(IV) complexes in A2780 cells, while the substitution of the second axial ligand with DCA resulted in significant increase in Pt cellular accumulation, perhaps due to higher lipophilicity of **2b**, consistent with its longer HPLC retention time (12.3 min for **2a**, 19.7 min for **2b**, Fig. S1, ESI†). Notably, the amount of Pt taken up by A2780 cells incubated with **1**, **2a** and **2b** was inversely proportional to their IC_{50} values. These results suggested that cellular accumulation of Pt(IV) prodrugs plays an important role in their antiproliferative activity. Since the avidin–**2a** complex exhibited improved photocytotoxicity, the effect of avidin on the uptake of **2a** was also investigated.

Table 2 Cellular Pt accumulation in A2780 ovarian cancer cells after exposure to complexes **2a**, **2b** and **1**, and the effect of avidin (10 μM Pt complex, 1 h incubation in the dark)

Pt accumulation (ng per 10^6 cells)[a]			
Complex		Complex with avidin	
2a	0.40 ± 0.15*	**2a**–avi (4 : 1)	4.1 ± 0.7*
2b	21.1 ± 2.0***	**2b**–avi (4 : 1)	20.0 ± 1.5***
1	0.64 ± 0.07***	**1**–avi (4 : 1)	0.56 ± 0.09**

[a] All experiments were conducted in triplicate. Comparison with untreated controls was performed by a two-tail *t*-test with unequal variances. $*p < 0.05$, $**p < 0.01$, $***p < 0.005$.

The accumulation of Pt after exposure of A2780 cells to the mixture of 10 μM **2a** and avidin (4 : 1) was 10× higher than **2a** alone, which correlates with the higher photocytotoxicity of **2a**–avidin complex. However, Pt accumulation for **1** and **2b** was not affected by avidin, since **1** does not contain biotin and **2b** is mainly taken up by passive diffusion due to its high lipophilicity.

A2780 ovarian cancer cells were treated with **2a** (1 or 2× photo IC_{50} concentration) in the presence and absence of light and live-imaged using confocal microscopy and flow cytometry to investigate changes in cell morphology (Fig. 3 and Fig. S8, S10, ESI†). The cell permeant dye SYTO™ 17 was used to stain the nuclei. Without irradiation, **2a** exhibited low cytotoxicity (IC_{50} > 100 μM) and, accordingly, no changes in cellular morphology were observed when cells were treated with **2a** for 2 h in the dark. In these conditions, the cells appeared healthy with well-defined plasma membranes and intact nuclei. In contrast, A2780 cells treated with **2a** exhibited dramatic morphological changes after 1 h irradiation with blue light (465 nm). The cells rounded up and the nuclei were fragmented into pieces. Damaged membranes and copious cell debris were observed when cells were treated with **2a** at 2 × IC_{50} concentration (Fig. 3 and Fig. S10, ESI†). DNA is usually regarded as the major target of platinum anticancer drugs, so the ability of **2a** to fragment cell nuclei exclusively upon irradiation, indicated its potential as a photoactive prodrug with a novel mechanism of action. Complex **2a** at higher concentration induced more morphological changes upon irradiation, while irradiation alone did not result in significant effects on cell morphology (Fig. S9 and S10, ESI†).

Cellular ROS generation for **2a**, **2b** and **1** was monitored in A549 lung cancer cells by DCFH-DA, which exhibits switch-on fluorescence in the presence of ROS. Cells treated with complexes (10 μM) in the dark showed no apparent change, but **2b** induced an increased DCF fluorescence upon irradiation, indicating its ability to generate ROS (Table S2, ESI†).

In summary, two novel biotinylated Pt(IV) complexes *trans*,-*trans*,*trans*-[$Pt(py)_2(N_3)_2$(biotin)(OH)] (**2a**) and *trans*,*trans*,*trans*-[$Pt(py)_2(N_3)_2$(biotin)(DCA)] (**2b**) have been synthesised and characterised. They exhibited good dark stability and promising

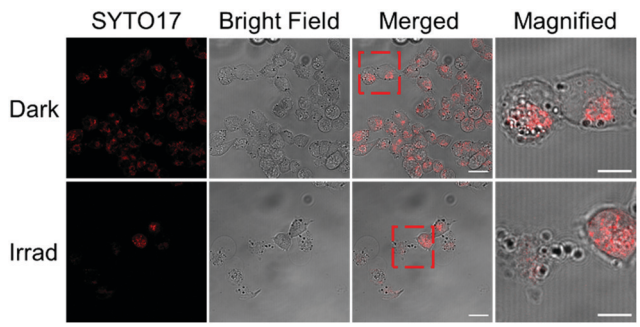

Fig. 3 Fluorescence images of A2780 ovarian cancer cells treated with **2a** (2 × photo IC_{50} concentration) in the dark and after irradiation with blue light (λ = 465 nm). Cells were stained by SYTO™ 17 (2.5 μM, $\lambda_{ex}/\lambda_{em}$ = 633/638–759 nm) for 30 min. Scale bar = 20 μm (10 μm in magnification). Fragmented nuclei and damaged membranes of A2780 cells treated with **2a** were observed upon irradiation, while in the dark, cells were intact and well-defined.

photoactivity, releasing azidyl radicals and generating singlet oxygen. Photoreactions with 5′-GMP resulted in the formation of $[Pt^{II}(CH_3CN)(py)_2(GMP\text{-}H)]^+$ as a major product. An increase in ct-DNA melting temperature suggested formation of inter-strand crosslinks. Promising photocytotoxicity of **2a** and **2b** towards human A2780 ovarian, A549 lung and PC3 prostate cancer cells was observed upon irradiation with low-dose blue light (465 nm, 4.8 mW cm^{-2}, 1 h), with high photocytotoxicity indices. The di-substituted **2b** exhibited much higher photocytotoxicity and cellular Pt accumulation, compared with mono-substituted **2a** and unsubstituted **1**. The strong interaction of **2a** and **2b** with avidin was confirmed by HABA displacement from avidin–HABA. When A2780 ovarian cancer cells were incubated with 1 : 4 avidin : **2a**, both photocytotoxicity and cellular accumulation increased significantly. Dramatic morphological changes in A2780 cells were observed after irradiation with **2a**, consistent with its promising photocytotoxicity.

We acknowledge financial support from the EPSRC (EP/G006792, EP/F034210/1 to PJS), University of Warwick (Chancellor's International PhD Scholarship for HS), Royal Society (grant no. NF160307, Newton International Fellowship for HH), and Wellcome Trust (grant no. 209173/Z/17/Z, Si Henry Wellcome Fellowship for CI).

Conflicts of interest

There are no conflicts to declare.

Notes and references

1 D. L. Ma, D. S. H. Chan and C. H. Leung, *Chem. Soc. Rev.*, 2013, **42**, 2130–2141.
2 L. Cai, Z. Gu, J. Zhong, D. Wen, G. Chen, L. He, J. Wu and Z. Gu, *Drug Discovery Today*, 2018, **23**, 1126–1138.
3 H. Ijaz, J. Qureshi, U. R. Tulain, F. Iqbal, Z. Danish, A. Fayyaz and A. Sethi, *Bioinspired, Biomimetic Nanobiomater.*, 2018, **7**, 109–121.
4 E. R. Ruskowitz and C. A. DeForest, *Nat. Rev. Mater.*, 2018, 17087.
5 W. X. Ren, J. Han, S. Uhm, Y. J. Jang, C. Kang, J. H. Kim and J. S. Kim, *Chem. Commun.*, 2015, **51**, 10403–10418.
6 J. Zempleni and D. M. Mock, *Am. J. Physiol.*, 1998, **275**, C382–C388.
7 K. Balamurugan, A. Ortiz and H. M. Said, *Am. J. Physiol.*, 2003, **285**, G73–G77.
8 P. D. Prasad, H. Wang, W. Huang, Y. J. Fei, F. H. Leibach, L. D. Devoe and V. Ganapathy, *Arch. Biochem. Biophys.*, 1999, **366**, 95–106.
9 S. Luo, V. S. Kansara, X. Zhu, D. Pal and A. K. Mitra, *Mol. Pharming*, 2006, **3**, 329–339.
10 H. Wang, W. Huang, W. Fei, H. Xia, T. L. Y. Feng, F. H. Leibac, L. D. Devoe, V. Ganapathy and P. D. Prasad, *J. Biol. Chem.*, 1999, **274**, 14875–14883.
11 N. M. Green, *Adv. Protein Chem.*, 1975, **29**, 85–133.
12 H. P. Lesch, M. U. Kaikkonen, J. T. Pikkarainen and S. Ylä-Herttuala, *Expert Opin. Drug Delivery*, 2010, **7**, 551–564.
13 X. Zeng, Y. Sun, X. Zhang and R. Zhuo, *Org. Biomol. Chem.*, 2009, **7**, 4201–4210.
14 A. Jain and K. Cheng, *J. Controlled Release*, 2017, **245**, 27–40.
15 S. C. Park, Y. M. Kim, N. H. Kim, E. J. Kim, Y. H. Park, J. R. Lee and M. K. Jang, *Macromol. Res.*, 2017, **25**, 882–889.
16 L. Chen, B. Schechter, R. Arnon and M. Wilchek, *Drug Dev. Res.*, 2000, **50**, 258–271.
17 N. Muhammad, N. Sadia, C. Zhu, C. Luo, Z. Guo and X. Wang, *Chem. Commun.*, 2017, **53**, 9971–9974.
18 S. Maiti, N. Park, J. H. Han, H. M. Jeon, J. H. Lee, S. Bhuniya, C. Kang and J. S. Kim, *J. Am. Chem. Soc.*, 2013, **135**, 4567–4572.
19 K. Li, L. Qiu, Q. Liu., G. Lv, X. Zhao, S. Wang and J. Lin, *J. Photochem. Photobiol., B*, 2017, **174**, 243–250.
20 B. Siewert, M. Langerman, A. Pannwitz and S. Bonnet, *Eur. J. Inorg. Chem.*, 2018, 4117–4124.
21 J. Li, L. Zeng, K. Xiong, T. W. Rees, C. Jin, W. Wu, Y. Chen, L. Jia and H. Chao, *Chem. Commun.*, 2019, **55**, 10972–10975.
22 B. Ghazal, E. N. Kaya, A. Husain, A. Ganesan, M. Durmuş, S. Makhseed and J. Porphyr, *Phthalocyanines*, 2019, **23**, 46–55.
23 S. Bonnet, *Dalton Trans.*, 2018, **47**, 10330–10343.
24 A. Bjelosevic, B. J. Pages, L. K. Spare, K. M. Deo, D. L. Ang and J. R. Aldrich-Wright, *Curr. Med. Chem.*, 2018, **25**, 478–492.
25 P. Müller, B. Schröder, J. A. Parkinson, N. A. Kratochwil, R. A. Coxall, A. Parkin, S. Parsons and P. J. Sadler, *Angew. Chem., Int. Ed.*, 2003, **42**, 335–339.
26 F. S. Mackay, J. A. Woods, P. Heringová, J. Kašpárková, A. M. Pizarro, S. A. Moggach, S. Parsons, V. Brabec and P. J. Sadler, *Proc. Natl. Acad. Sci. U. S. A.*, 2007, **104**, 20743–20748.
27 N. J. Farrer, J. A. Woods, L. Salassa, Y. Zhao, K. S. Robinson, G. Clarkson, F. S. Mackay and P. J. Sadler, *Angew. Chem., Int. Ed.*, 2010, **49**, 8905–8908.
28 Y. Zhao, N. J. Farrer, H. Li, J. S. Butler, R. J. McQuitty, A. Habtemariam, F. Wang and P. J. Sadler, *Angew. Chem., Int. Ed.*, 2013, **52**, 13633–13637.
29 J. S. Butler, J. A. Woods, N. J. Farrer, M. E. Newton and P. J. Sadler, *J. Am. Chem. Soc.*, 2012, **134**, 16508–16511.
30 J. Pracharova, L. Zerzankova, J. Stepankova, O. Novakova, N. J. Farrer, P. J. Sadler, V. Brabec and J. Kasparkova, *Chem. Res. Toxicol.*, 2012, **25**, 1099–1111.
31 M. D. Hall and T. W. Hambley, *Coord. Chem. Rev.*, 2002, **232**, 49–67.
32 A. Gandioso, E. Shaili, A. Massaguer, G. Artigas, A. González-Cantó, J. A. Woods, P. J. Sadler and V. Marchán, *Chem. Commun.*, 2015, **51**, 9169–9172.
33 E. Shaili, M. Fernández-Giménez, S. Rodríguez-Astor, A. Gandioso, L. Sandín, C. García-Vélez, A. Massaguer, G. J. Clarkson, J. A. Woods, P. J. Sadler and V. Marchán, *Chem. – Eur. J.*, 2015, **21**, 18474–18486.
34 H. Shi, Q. Wang, V. Venkatesh, G. Feng, L. S. Young, I. Romero-Canelón, M. Zeng and P. J. Sadler, *Dalton Trans.*, 2019, **48**, 8560–8564.
35 E. Wexselblatt, E. Yavin and D. Gibson, *Angew. Chem., Int. Ed.*, 2013, **52**, 6059–6062.
36 S. Dhara and S. J. Lippard, *Proc. Natl. Acad. Sci. U. S. A.*, 2009, **106**, 22199–22204.
37 E. Petruzzella, J. P. Braude, J. R. Aldrich-Wright, V. Gandin and D. Gibson, *Angew. Chem., Int. Ed.*, 2017, **56**, 11539–11544.
38 R. R. Vernooij, T. Joshi, M. D. Horbury, B. Graham, E. I. Izgorodina, V. G. Stavros, P. J. Sadler, L. Spiccia and B. R. Wood, *Chem. – Eur. J.*, 2018, **24**, 5790–5803.
39 N. M. Green, *Biochem. J.*, 1965, **94**, 23c–24c.